Today's Outline - February 20, 2020

Today's Outline - February 20, 2020

- HW #02 solutions

Today's Outline - February 20, 2020

- HW #02 solutions
- Unified fit model

Today's Outline - February 20, 2020

- HW #02 solutions
- Unified fit model
- Interparticle interactions

Today's Outline - February 20, 2020

- HW #02 solutions
- Unified fit model
- Interparticle interactions
- SAXS papers

Today's Outline - February 20, 2020

- HW #02 solutions
- Unified fit model
- Interparticle interactions
- SAXS papers

Homework Assignment #03:
Chapter 3:1,3,4,6,8
due Thursday, February 27, 2020

HW #02

1. Knowing that the photoelectric absorption of an element scales as the inverse of the energy cubed, calculate:

(a) the absorption coefficient at 10keV for copper when the value at 5keV is 1698.3 cm^{-1};

(b) The actual absorption coefficient of copper at 10keV is 1942.1 cm^{-1}, why is this so different than your calculated value?

2. A 30 cm long, ionization chamber, filled with 80% helium and 20% nitrogen gases at 1 atmosphere, is being used to measure the photon rate (photons/sec) in a synchrotron beamline at 12 keV. If a current of 10 nA is measured, what is the photon flux entering the ionization chamber?

3. A 5 cm deep ionization chamber is used to measure the fluorescence from a sample containing arsenic (As). Using any noble gases or nitrogen, determine a gas fill (at 1 atmosphere) for this chamber which absorbs at least 60% of the incident photons. How does this change if you are measuring the fluorescence from ruthenium (Ru)?

HW #02

4. Calculate the critical angle of reflection of 10 keV and 30 keV x-rays for:

(a) A slab of glass (SiO_2);

(b) A thick chromium mirror;

(c) A thick platinum mirror.

(d) If the incident x-ray beam is 2 mm high, what length of mirror is required to reflect the entire beam for each material?

5. Calculate the fraction of silver (Ag) fluorescence x-rays which are absorbed in a 1 mm thick silicon (Si) detector and the charge pulse expected for each absorbed photon. Repeat the calculation for a 1 mm thick germanium (Ge) detector.

SAXS review

The SAXS scattered intensity from a dilute solution depends on the single particle form factor, $\mathcal{F}(\vec{Q})$, the volume of the particle, V_p, and the density difference from the solvent, $\Delta\rho = (\rho_{sl,p} - \rho_{sl,0})$

SAXS review

The SAXS scattered intensity from a dilute solution depends on the single particle form factor, $\mathcal{F}(\vec{Q})$, the volume of the particle, V_p, and the density difference from the solvent, $\Delta\rho = (\rho_{sl,p} - \rho_{sl,0})$

$$I^{SAXS}(\vec{Q}) = \Delta\rho^2 V_p^2 |\mathcal{F}(\vec{Q})|^2$$

SAXS review

The SAXS scattered intensity from a dilute solution depends on the single particle form factor, $\mathcal{F}(\vec{Q})$, the volume of the particle, V_p, and the density difference from the solvent, $\Delta\rho = (\rho_{sl,p} - \rho_{sl,0})$

the long wavelength limit ($QR \rightarrow 0$) is called the Guinier regime and it is possible to extract the radius of gyration R_g of the particle

$$I^{SAXS}(\vec{Q}) = \Delta\rho^2 V_p^2 |\mathcal{F}(\vec{Q})|^2$$

SAXS review

The SAXS scattered intensity from a dilute solution depends on the single particle form factor, $\mathcal{F}(\vec{Q})$, the volume of the particle, V_p, and the density difference from the solvent, $\Delta\rho = (\rho_{sl,p} - \rho_{sl,0})$

the long wavelength limit ($QR \rightarrow 0$) is called the Guinier regime and it is possible to extract the radius of gyration R_g of the particle

$$I^{SAXS}(\vec{Q}) = \Delta\rho^2 V_p^2 |\mathcal{F}(\vec{Q})|^2$$

$$I^{SAXS}(Q) \approx \Delta\rho^2 V_p^2 e^{-Q^2 R_g^2/3}$$

SAXS review

The SAXS scattered intensity from a dilute solution depends on the single particle form factor, $\mathcal{F}(\vec{Q})$, the volume of the particle, V_p, and the density difference from the solvent, $\Delta\rho = (\rho_{sl,p} - \rho_{sl,0})$

the long wavelength limit ($QR \rightarrow 0$) is called the Guinier regime and it is possible to extract the radius of gyration R_g of the particle

$$I^{SAXS}(\vec{Q}) = \Delta\rho^2 V_p^2 |\mathcal{F}(\vec{Q})|^2$$

$$I^{SAXS}(Q) \approx \Delta\rho^2 V_p^2 e^{-Q^2 R_g^2/3}$$

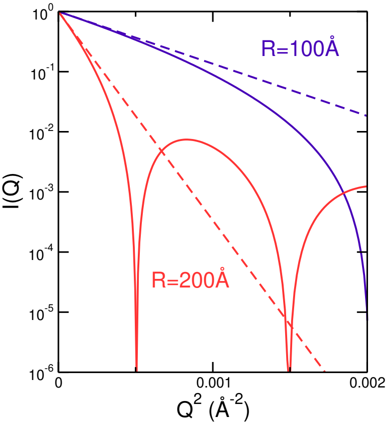

The SAXS scattered intensity from a dilute solution depends on the single particle form factor, $\mathcal{F}(\vec{Q})$, the volume of the particle, V_p, and the density difference from the solvent, $\Delta\rho = (\rho_{sl,p} - \rho_{sl,0})$

the long wavelength limit ($QR \rightarrow 0$) is called the Guinier regime and it is possible to extract the radius of gyration R_g of the particle

$$R_g^2 = \frac{\int_{V_p} \rho_{sl,p}(\vec{r}) r^2 dV_p}{\int_{V_p} \rho_{sl,p}(\vec{r}) dV_p}$$

$$I^{SAXS}(\vec{Q}) = \Delta\rho^2 V_p^2 |\mathcal{F}(\vec{Q})|^2$$

$$I^{SAXS}(Q) \approx \Delta\rho^2 V_p^2 e^{-Q^2 R_g^2/3}$$

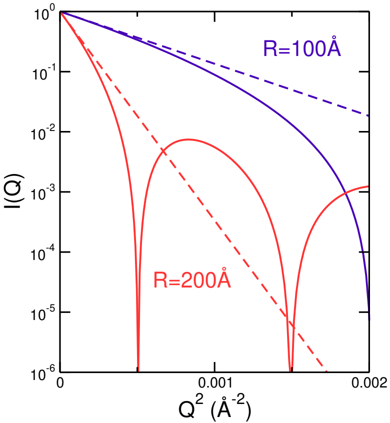

Unified model for SAXS

For inhomogeneous samples, using simple Guinier and Porod models can give an incorrect description of the actual sample

Unified model for SAXS

For inhomogeneous samples, using simple Guinier and Porod models can give an incorrect description of the actual sample

This can be solved, judiciously, using the Unified model proposed by Beaucage in 1995

Unified model for SAXS

For inhomogeneous samples, using simple Guinier and Porod models can give an incorrect description of the actual sample

This can be solved, judiciously, using the Unified model proposed by Beaucage in 1995

The idea is to include multiple populations each with its own Guinier dependence with R_g and a power law dependence that asymptotically approaches the Porod law for spheres

Unified model for SAXS

For inhomogeneous samples, using simple Guinier and Porod models can give an incorrect description of the actual sample

This can be solved, judiciously, using the Unified model proposed by Beaucage in 1995

The idea is to include multiple populations each with its own Guinier dependence with R_g and a power law dependence that asymptotically approaches the Porod law for spheres

$$I(q) = B_{bkg} + \sum_{i=1}^{N} G_i e^{-\frac{q^2 R_{g,i}^2}{3}} + e^{-\frac{q^2 R_{g,i-1}^2}{3}} B_i \left[\frac{\left(erf \left\{ \frac{q R_{g,i}}{\sqrt{6}} \right\} \right)^3}{q} \right]^{P_i}$$

Unified model for SAXS

For inhomogeneous samples, using simple Guinier and Porod models can give an incorrect description of the actual sample

This can be solved, judiciously, using the Unified model proposed by Beaucage in 1995

The idea is to include multiple populations each with its own Guinier dependence with R_g and a power law dependence that asymptotically approaches the Porod law for spheres

$$I(q) = B_{bkg} + \sum_{i=1}^{N} G_i e^{-\frac{q^2 R_{g,i}^2}{3}} + e^{-\frac{q^2 R_{g,i-1}^2}{3}} B_i \left[\frac{\left(erf \left\{ \frac{qR_{g,i}}{\sqrt{6}} \right\} \right)^3}{q} \right]^{P_i}$$

The sum is over structural levels starting with the smallest. For each level there is a Guinier exponential prefactor (G_i), a radius of gyration ($R_{g,i}$), a power law constant prefactor (B_i), and a power law exponent (P_i).

Unified model for SAXS

$$I(q) = B_{bkg} + \sum_{i=1}^{N} G_i e^{-\frac{q^2 R_{g,i}^2}{3}} + e^{-\frac{q^2 R_{g,i-1}^2}{3}} B_i \left[\frac{\left(erf \left\{ \frac{q R_{g,i}}{\sqrt{6}} \right\} \right)^3}{q} \right]^{P_i}$$

Unified model for SAXS

$$I(q) = B_{bkg} + \sum_{i=1}^{N} G_i e^{-\frac{q^2 R_{g,i}^2}{3}} + e^{-\frac{q^2 R_{g,i-1}^2}{3}} B_i \left[\frac{\left(erf\left\{ \frac{q R_{g,i}}{\sqrt{6}} \right\} \right)^3}{q} \right]^{P_i}$$

$R_{g,i-1}$ is the high-q power law cutoff for each level and is taken to be the radius of gyration of the previous level to avoid double counting.

Unified model for SAXS

$$I(q) = B_{bkg} + \sum_{i=1}^{N} G_i e^{-\frac{q^2 R_{g,i}^2}{3}} + e^{-\frac{q^2 R_{g,i-1}^2}{3}} B_i \left[\frac{\left(erf \left\{ \frac{q R_{g,i}}{\sqrt{6}} \right\} \right)^3}{q} \right]^{P_i}$$

$R_{g,i-1}$ is the high-q power law cutoff for each level and is taken to be the radius of gyration of the previous level to avoid double counting.

Additional parameters can be added, such as a structure factor that is different than unity, and interparticle correlation parameters.

Unified model for SAXS

$$I(q) = B_{bkg} + \sum_{i=1}^{N} G_i e^{-\frac{q^2 R_{g,i}^2}{3}} + e^{-\frac{q^2 R_{g,i-1}^2}{3}} B_i \left[\frac{\left(erf \left\{ \frac{q R_{g,i}}{\sqrt{6}} \right\} \right)^3}{q} \right]^{P_i}$$

$R_{g,i-1}$ is the high-q power law cutoff for each level and is taken to be the radius of gyration of the previous level to avoid double counting.

Additional parameters can be added, such as a structure factor that is different than unity, and interparticle correlation parameters.

It is important not to include more levels than are significant physically

Inter-particle interactions

Many interesting problems fall outside the dilute limit.

Inter-particle interactions

Many interesting problems fall outside the dilute limit.

In these cases, the SAXS modeling must include not only the particle form factor but an additional structure factor, $S(Q)$

Inter-particle interactions

Many interesting problems fall outside the dilute limit.

In these cases, the SAXS modeling must include not only the particle form factor but an additional structure factor, $S(Q)$

$$I^{SAXS}(Q) = \Delta\rho^2 V_p^2 |\mathcal{F}(\vec{Q})|^2 S(Q)$$

Inter-particle interactions

Many interesting problems fall outside the dilute limit.

In these cases, the SAXS modeling must include not only the particle form factor but an additional structure factor, $S(Q)$

$$I^{SAXS}(Q) = \Delta\rho^2 V_p^2 |\mathcal{F}(\vec{Q})|^2 S(Q)$$

The book has an example of this and we will look at a couple of others from recent journal articles

Inter-particle interactions

Many interesting problems fall outside the dilute limit.

In these cases, the SAXS modeling must include not only the particle form factor but an additional structure factor, $S(Q)$

$$I^{SAXS}(Q) = \Delta\rho^2 V_p^2 |\mathcal{F}(\vec{Q})|^2 S(Q)$$

The book has an example of this and we will look at a couple of others from recent journal articles

- SAXS of irradiated Zn nanoparticles

Inter-particle interactions

Many interesting problems fall outside the dilute limit.

In these cases, the SAXS modeling must include not only the particle form factor but an additional structure factor, $S(Q)$

$$I^{SAXS}(Q) = \Delta\rho^2 V_p^2 |\mathcal{F}(\vec{Q})|^2 S(Q)$$

The book has an example of this and we will look at a couple of others from recent journal articles

- SAXS of irradiated Zn nanoparticles
- Nucleation and growth of & glycine crystals

SAXS of irradiated Zn nanoparticles

Zn nanoparticles formed in SiO_2 by ion implantation are irradiated with high energy Xe^{+14} ions.

"Shape elongation of embedded Zn nanoparticles induced by swift heavy ion irradiation: A SAXS study", H. Amekura, K. Kono, N. Okubo, and N. Ishikawa, *Phys. Status Solidi B* **252**, 165-169 (2015).

SAXS of irradiated Zn nanoparticles

Zn nanoparticles formed in SiO_2 by ion implantation are irradiated with high energy Xe^{+14} ions.

SAXS is measured using 18 keV x-rays both parallel and perpendicular to the direction of Xe^{+14} irradiation.

"Shape elongation of embedded Zn nanoparticles induced by swift heavy ion irradiation: A SAXS study", H. Amekura, K. Kono, N. Okubo, and N. Ishikawa, *Phys. Status Solidi B* **252**, 165-169 (2015).

SAXS of irradiated Zn nanoparticles

Zn nanoparticles formed in SiO_2 by ion implantation are irradiated with high energy Xe^{+14} ions.

SAXS is measured using 18 keV x-rays both parallel and perpendicular to the direction of Xe^{+14} irradiation.

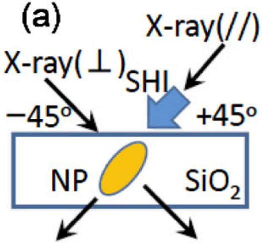

Expt. geometry

"Shape elongation of embedded Zn nanoparticles induced by swift heavy ion irradiation: A SAXS study", H. Amekura, K. Kono, N. Okubo, and N. Ishikawa, *Phys. Status Solidi B* **252**, 165-169 (2015).

SAXS of irradiated Zn nanoparticles

Zn nanoparticles formed in SiO_2 by ion implantation are irradiated with high energy Xe^{+14} ions.

SAXS is measured using 18 keV x-rays both parallel and perpendicular to the direction of Xe^{+14} irradiation.

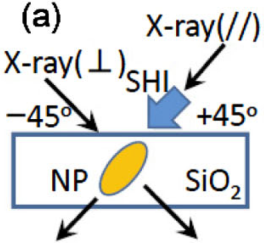

Expt. geometry

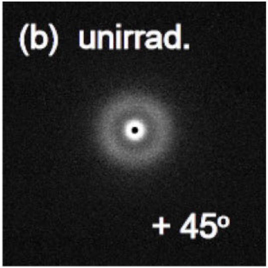

Unirradiated

"Shape elongation of embedded Zn nanoparticles induced by swift heavy ion irradiation: A SAXS study", H. Amekura, K. Kono, N. Okubo, and N. Ishikawa, *Phys. Status Solidi B* **252**, 165-169 (2015).

SAXS of irradiated Zn nanoparticles

Zn nanoparticles formed in SiO_2 by ion implantation are irradiated with high energy Xe^{+14} ions.

SAXS is measured using 18 keV x-rays both parallel and perpendicular to the direction of Xe^{+14} irradiation.

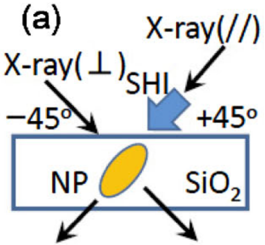

Expt. geometry

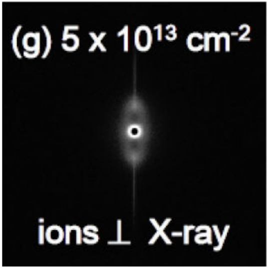

Irradiated ⊥ x-rays

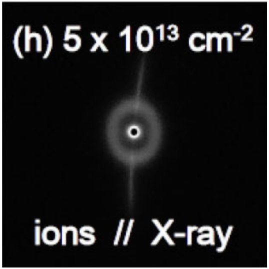

Irradiated ∥ x-rays

"Shape elongation of embedded Zn nanoparticles induced by swift heavy ion irradiation: A SAXS study", H. Amekura, K. Kono, N. Okubo, and N. Ishikawa, *Phys. Status Solidi B* **252**, 165-169 (2015).

SAXS of irradiated Zn nanoparticles

Zn nanoparticles formed in SiO_2 by ion implantation are irradiated with high energy Xe^{+14} ions.

SAXS is measured using 18 keV x-rays both parallel and perpendicular to the direction of Xe^{+14} irradiation.

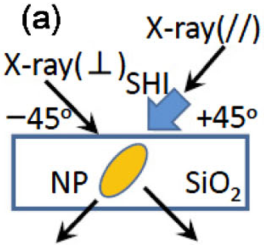

Expt. geometry

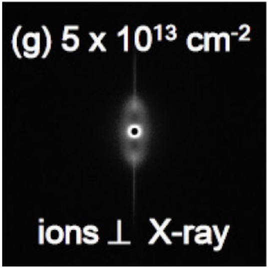

Irradiated ⊥ x-rays

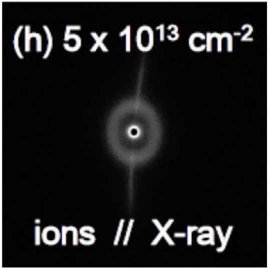

Irradiated ∥ x-rays

Straight lines are due to ion tracks, seen in both directions and which persist to the highest fluences.

"Shape elongation of embedded Zn nanoparticles induced by swift heavy ion irradiation: A SAXS study", H. Amekura, K. Kono, N. Okubo, and N. Ishikawa, *Phys. Status Solidi B* **252**, 165-169 (2015).

SAXS of irradiated Zn nanoparticles

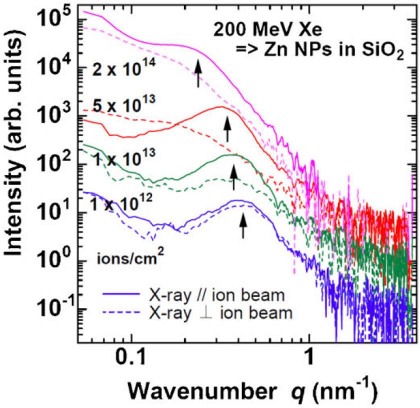

Interference peak persists for $\parallel$ but not $\perp$ incidence

"Shape elongation of embedded Zn nanoparticles induced by swift heavy ion irradiation: A SAXS study", H. Amekura, K. Kono, N. Okubo, and N. Ishikawa, *Phys. Status Solidi B* **252**, 165-169 (2015).

SAXS of irradiated Zn nanoparticles

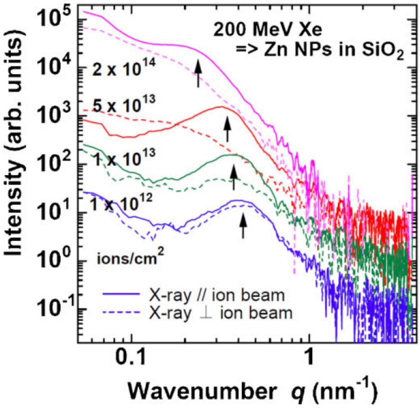

Interference peak persists for ∥ but not ⊥ incidence

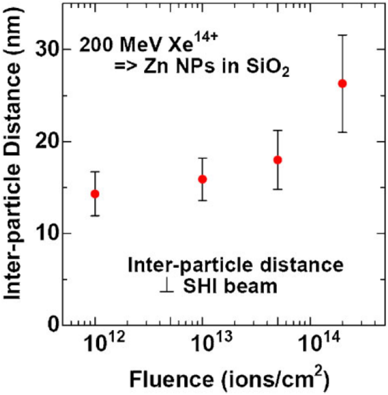

Interparticle distance increases as a function of irradiation fluence

"Shape elongation of embedded Zn nanoparticles induced by swift heavy ion irradiation: A SAXS study", H. Amekura, K. Kono, N. Okubo, and N. Ishikawa, *Phys. Status Solidi B* **252**, 165-169 (2015).

SAXS of irradiated Zn nanoparticles

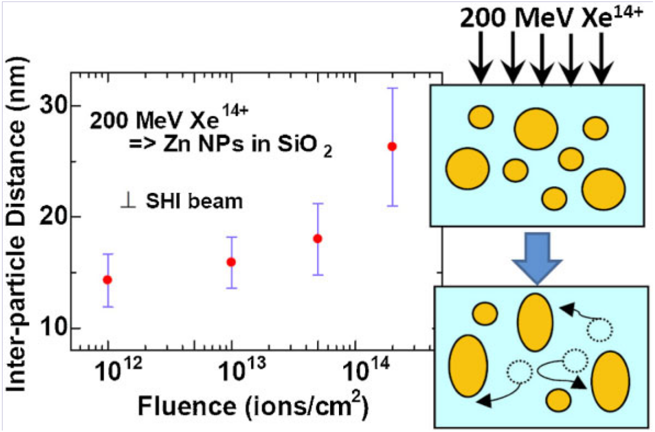

"Shape elongation of embedded Zn nanoparticles induced by swift heavy ion irradiation: A SAXS study", H. Amekura, K. Kono, N. Okubo, and N. Ishikawa, *Phys. Status Solidi B* **252**, 165-169 (2015).

SAXS of irradiated Zn nanoparticles

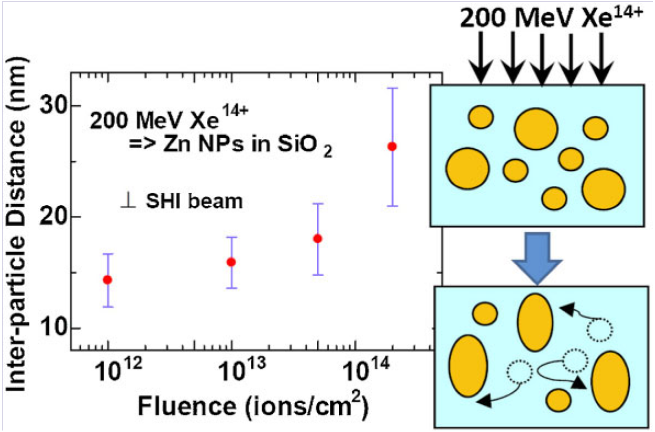

Growth of interparticle spacing is due to dissolution and re-agglomeration with fluence leading to larger interparticle spacings

"Shape elongation of embedded Zn nanoparticles induced by swift heavy ion irradiation: A SAXS study", H. Amekura, K. Kono, N. Okubo, and N. Ishikawa, *Phys. Status Solidi B* **252**, 165-169 (2015).

Nucleation & growth of glycine

Can SAXS help us understand the nucleation and growth of a simple molecule which is the prototype for pharmaceutical compounds?

"SAXS study of the nucleation of glycine crystals from a supersaturated solution," S. Chattopadhyay et al. *Crystal Growth Design* **5**, 523-527 (2004)

Nucleation & growth of glycine

Can SAXS help us understand the nucleation and growth of a simple molecule which is the prototype for pharmaceutical compounds?

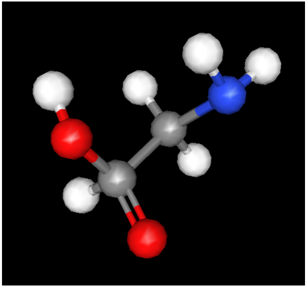

"SAXS study of the nucleation of glycine crystals from a supersaturated solution," S. Chattopadhyay et al. *Crystal Growth Design* **5**, 523-527 (2004)

Nucleation & growth of glycine

Can SAXS help us understand the nucleation and growth of a simple molecule which is the prototype for pharmaceutical compounds?

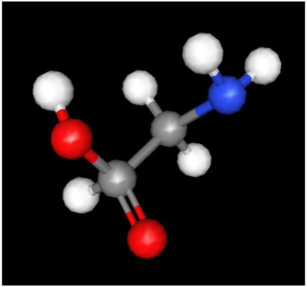

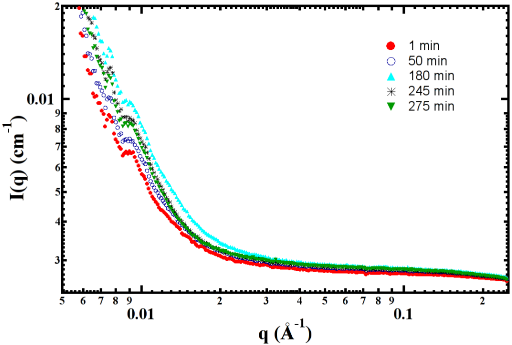

Initial studies at 12keV observe change in R_g upon crystallization.

"SAXS study of the nucleation of glycine crystals from a supersaturated solution," S. Chattopadhyay et al. *Crystal Growth Design* **5**, 523-527 (2004)

Nucleation & growth of glycine

Can SAXS help us understand the nucleation and growth of a simple molecule which is the prototype for pharmaceutical compounds?

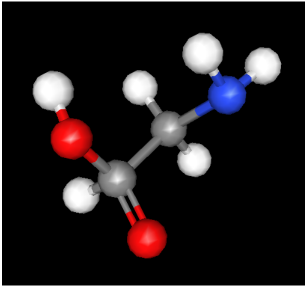

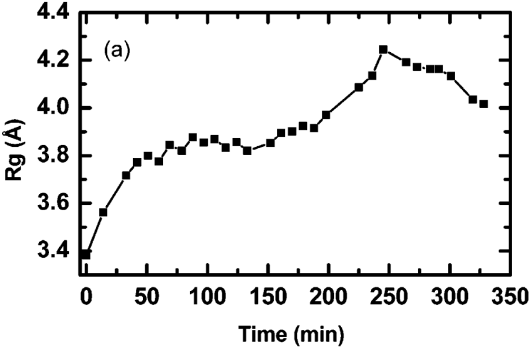

Initial studies at 12keV observe change in R_g upon crystallization. Results confirm a two-step model of cystallization and dimerization in aqueous solution.

"SAXS study of the nucleation of glycine crystals from a supersaturated solution," S. Chattopadhyay et al. *Crystal Growth Design* **5**, 523-527 (2004)

Can SAXS help us understand the nucleation and growth of a simple molecule which is the prototype for pharmaceutical compounds?

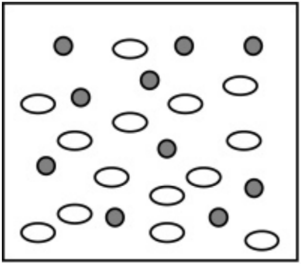

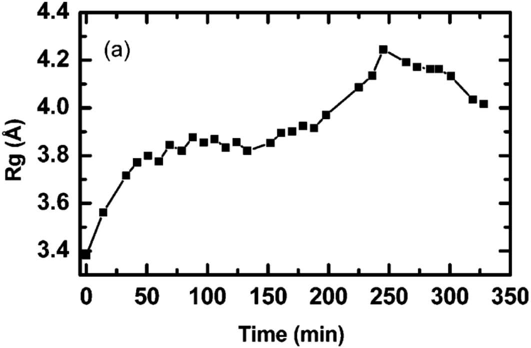

Initial studies at 12keV observe change in R_g upon crystallization. Results confirm a two-step model of cystallization and dimerization in aqueous solution.

"SAXS study of the nucleation of glycine crystals from a supersaturated solution," S. Chattopadhyay et al. *Crystal Growth Design* **5**, 523-527 (2004)

Nucleation & growth of glycine

Can SAXS help us understand the nucleation and growth of a simple molecule which is the prototype for pharmaceutical compounds?

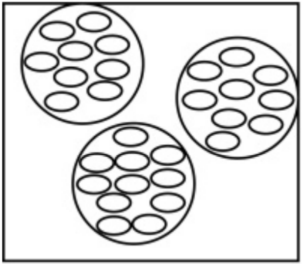

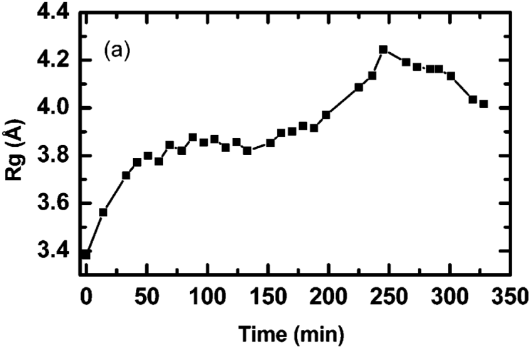

Initial studies at 12keV observe change in R_g upon crystallization. Results confirm a two-step model of cystallization and dimerization in aqueous solution.

"SAXS study of the nucleation of glycine crystals from a supersaturated solution," S. Chattopadhyay et al. *Crystal Growth Design* **5**, 523-527 (2004)

Nucleation & growth of glycine

Can SAXS help us understand the nucleation and growth of a simple molecule which is the prototype for pharmaceutical compounds?

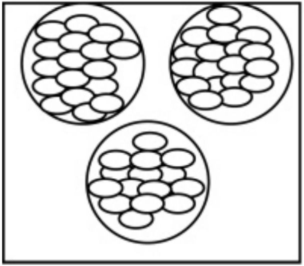

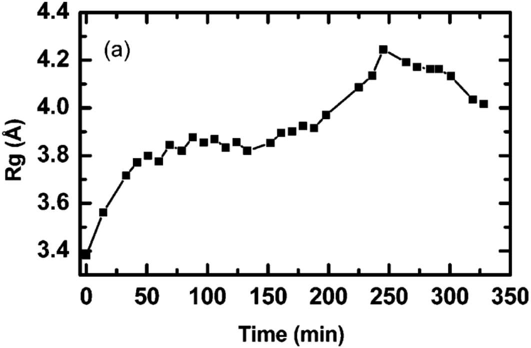

Initial studies at 12keV observe change in R_g upon crystallization. Results confirm a two-step model of cystallization and dimerization in aqueous solution.

"SAXS study of the nucleation of glycine crystals from a supersaturated solution," S. Chattopadhyay et al. *Crystal Growth Design* **5**, 523-527 (2004)

Glycine nucleation

Long nucleation times due to heating from absorbed 12 keV x-rays.

Glycine nucleation

Long nucleation times due to heating from absorbed 12 keV x-rays.

Change to 25 keV x-rays reduces crystallization time to under 90 min

Glycine nucleation

Long nucleation times due to heating from absorbed 12 keV x-rays.

Change to 25 keV x-rays reduces crystallization time to under 90 min

Different polymorphs are produced under varying conditions so study extended to both neutral and acidic solutions

Glycine nucleation

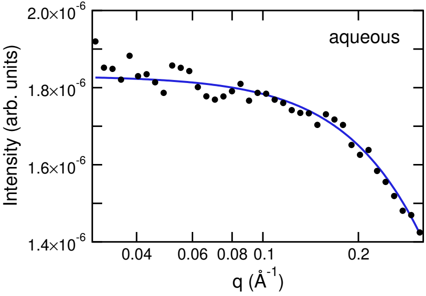

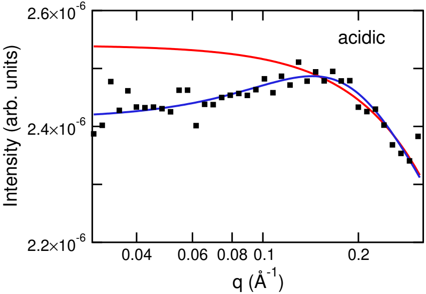

Long nucleation times due to heating from absorbed 12 keV x-rays.

Change to 25 keV x-rays reduces crystallization time to under 90 min

Different polymorphs are produced under varying conditions so study extended to both neutral and acidic solutions

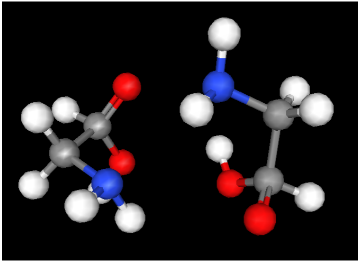

Glycine nucleation

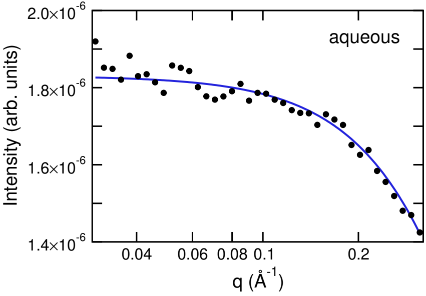

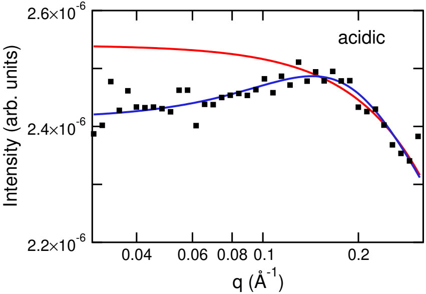

Long nucleation times due to heating from absorbed 12 keV x-rays.

Change to 25 keV x-rays reduces crystallization time to under 90 min

Different polymorphs are produced under varying conditions so study extended to both neutral and acidic solutions

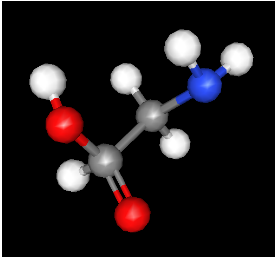

Glycine R_g

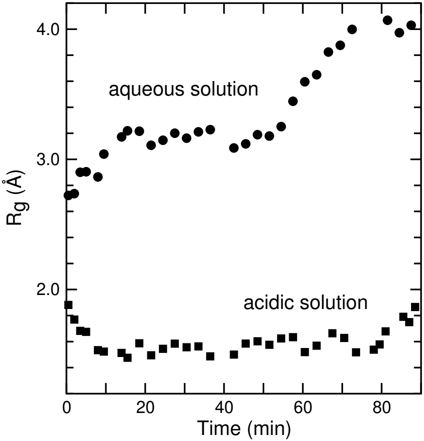

in aqueous solution, R_g implies dimerization and increases due to aggregation until crystallization

in acidic solution, Rg remains small and implies that no dimerization or aggregation occurs before nucleation

"Relationship between self-sssociation of glycine molecules in supersaturated solution and solid state outcome", D. Erdemir et al. *Phys. Rev. Lett.* **99**, 115702 (2007)

Size exclusion chromatography SAXS

SAXS of biological molecules is an excellent way of getting some information about the molecules as they exist in solution.

Size exclusion chromatography SAXS

SAXS of biological molecules is an excellent way of getting some information about the molecules as they exist in solution.

Obtaining information about R_g and the Porod region, combined with modeling and the known crystallographic structures can give a more complete picture of how these molecules function.

Size exclusion chromatography SAXS

SAXS of biological molecules is an excellent way of getting some information about the molecules as they exist in solution.

Obtaining information about R_g and the Porod region, combined with modeling and the known crystallographic structures can give a more complete picture of how these molecules function.

A major problem in these systems is aggregation and impurities. Pre-purification of samples is important but if they are left for some time before the SAXS mefasurement is performed, there can be decomposition.

Size exclusion chromatography SAXS

SAXS of biological molecules is an excellent way of getting some information about the molecules as they exist in solution.

Obtaining information about R_g and the Porod region, combined with modeling and the known crystallographic structures can give a more complete picture of how these molecules function.

A major problem in these systems is aggregation and impurities. Pre-purification of samples is important but if they are left for some time before the SAXS mefasurement is performed, there can be decomposition.

Even without any aggregation or decomposition, separation into a monodisperse molecule size is challenging.

Size exclusion chromatography SAXS

SAXS of biological molecules is an excellent way of getting some information about the molecules as they exist in solution.

Obtaining information about R_g and the Porod region, combined with modeling and the known crystallographic structures can give a more complete picture of how these molecules function.

A major problem in these systems is aggregation and impurities. Pre-purification of samples is important but if they are left for some time before the SAXS mefasurement is performed, there can be decomposition.

Even without any aggregation or decomposition, separation into a monodisperse molecule size is challenging.

Mathew, Mirza & Menhart, "Liquid-chromatography-coupled SAXS for accurate sizing of aggregating proteins," *J. Synchrotron Rad.* **11**, 314-318 (2004) developed a technique which is now being used routinely in biological SAXS, called Size Exclusion Chromatography SAXS.

Size exclusion chromatography SAXS

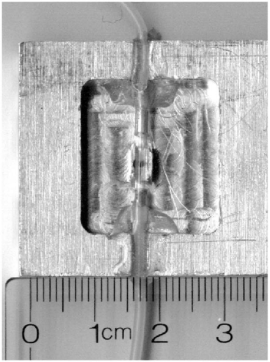

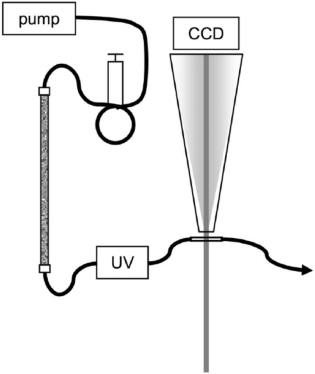

"Liquid-chromatography-coupled SAXS for accurate sizing of aggregating proteins," Mathew, Mirza & Menhart, *J. Synchrotron Rad.* **11**, 314-318 (2004).

Size exclusion chromatography SAXS

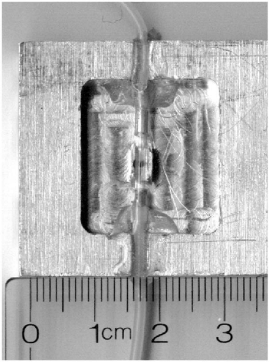

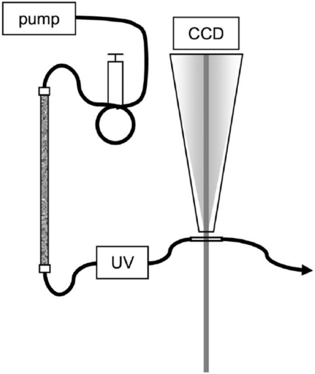

2m SAXS camera, 1.03Å (12 keV) x-rays were used

"Liquid-chromatography-coupled SAXS for accurate sizing of aggregating proteins," Mathew, Mirza & Menhart, *J. Synchrotron Rad.* **11**, 314-318 (2004).

Size exclusion chromatography SAXS

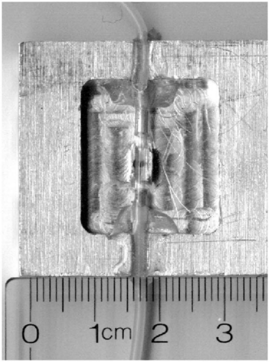

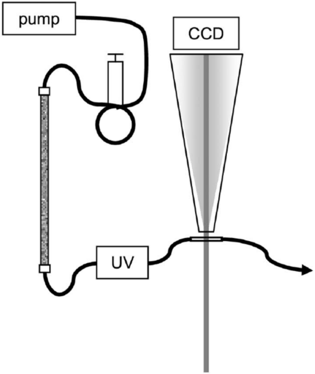

2m SAXS camera, 1.03Å (12 keV) x-rays were used

2s exposure times every 20s, with 0.25 ml/min flow rate

"Liquid-chromatography-coupled SAXS for accurate sizing of aggregating proteins," Mathew, Mirza & Menhart, *J. Synchrotron Rad.* **11**, 314-318 (2004).

Size exclusion chromatography SAXS

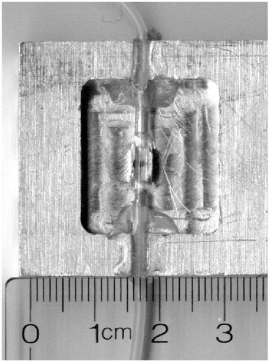

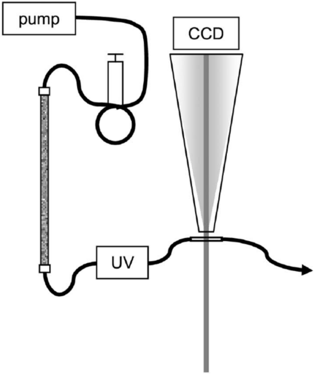

2m SAXS camera, 1.03Å (12 keV) x-rays were used

2s exposure times every 20s, with 0.25 ml/min flow rate

samples of (1) cytochrome c, (2) plasminogen, (3) mixture of cytochrome c bovine serum albumin, and blue dextran

"Liquid-chromatography-coupled SAXS for accurate sizing of aggregating proteins," Mathew, Mirza & Menhart, *J. Synchrotron Rad.* **11**, 314-318 (2004).

Cytochrome c

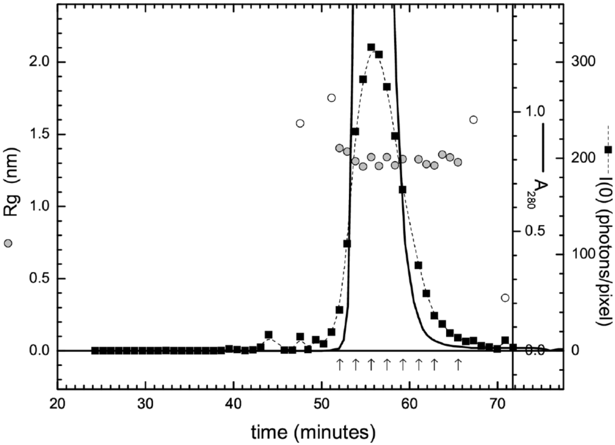

“Liquid-chromatography-coupled SAXS for accurate sizing of aggregating proteins,” Mathew, Mirza & Menhart, *J. Synchrotron Rad.* **11**, 314-318 (2004).

Cytochrome c

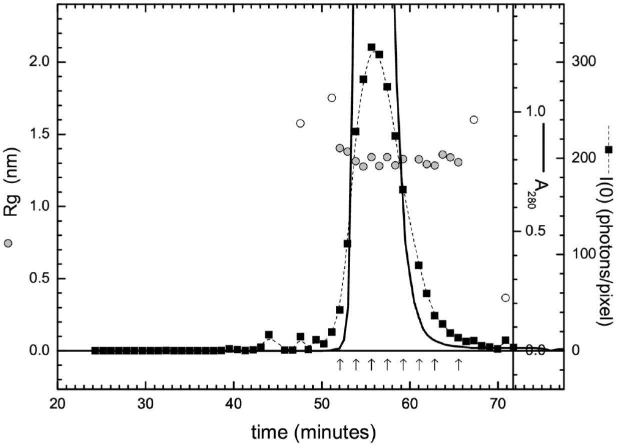

Forward scatter (black squares) gives a measure of the total number of electrons in the beam

"Liquid-chromatography-coupled SAXS for accurate sizing of aggregating proteins," Mathew, Mirza & Menhart, *J. Synchrotron Rad.* **11**, 314-318 (2004).

Cytochrome c

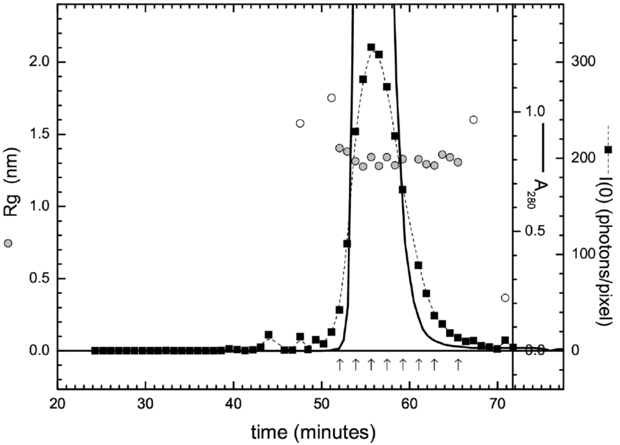

Forward scatter (black squares) gives a measure of the total number of electrons in the beam R_g is constant throughout the main peak.

"Liquid-chromatography-coupled SAXS for accurate sizing of aggregating proteins," Mathew, Mirza & Menhart, *J. Synchrotron Rad.* **11**, 314-318 (2004).

Cytochrome c - Guinier plots

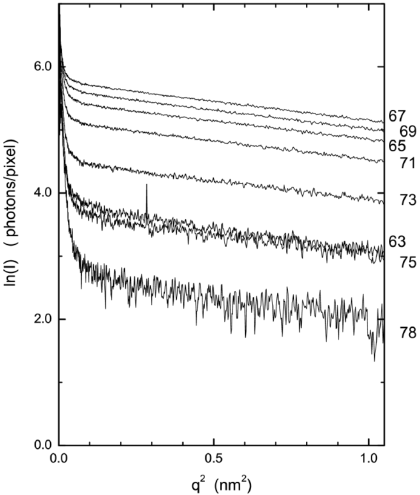

"Liquid-chromatography-coupled SAXS for accurate sizing of aggregating proteins," Mathew, Mirza & Menhart, *J. Synchrotron Rad.* **11**, 314-318 (2004).

Cytochrome c - Guinier plots

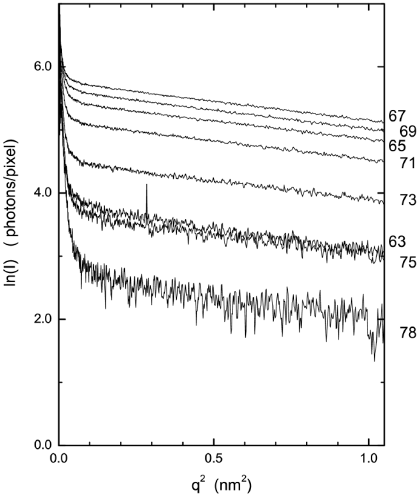

Plot from times marked with arrows on R_g plot.

"Liquid-chromatography-coupled SAXS for accurate sizing of aggregating proteins," Mathew, Mirza & Menhart, *J. Synchrotron Rad.* **11**, 314-318 (2004).

Cytochrome c - Guinier plots

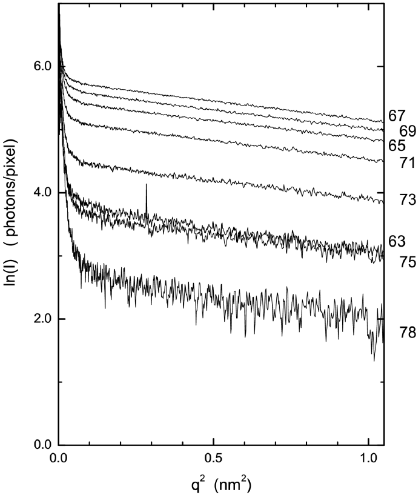

Plot from times marked with arrows on R_g plot.

Guinier plots are parallel, indicating a single species present (a single critical exponent).

"Liquid-chromatography-coupled SAXS for accurate sizing of aggregating proteins," Mathew, Mirza & Menhart, *J. Synchrotron Rad.* **11**, 314-318 (2004).

Cytochrome c - Guinier plots

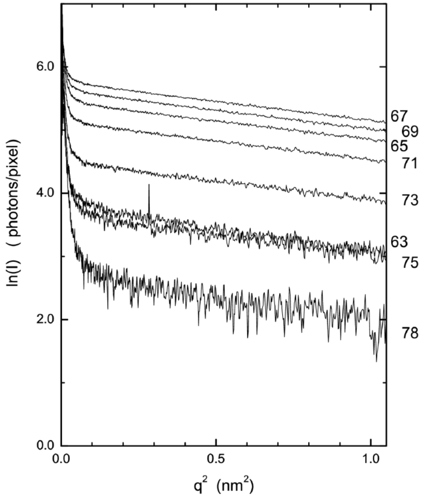

Plot from times marked with arrows on R_g plot.

Guinier plots are parallel, indicating a single species present (a single critical exponent).

Even lowest intensity data set gives a consistent R_g.

"Liquid-chromatography-coupled SAXS for accurate sizing of aggregating proteins," Mathew, Mirza & Menhart, *J. Synchrotron Rad.* **11**, 314-318 (2004).

Plasminogen

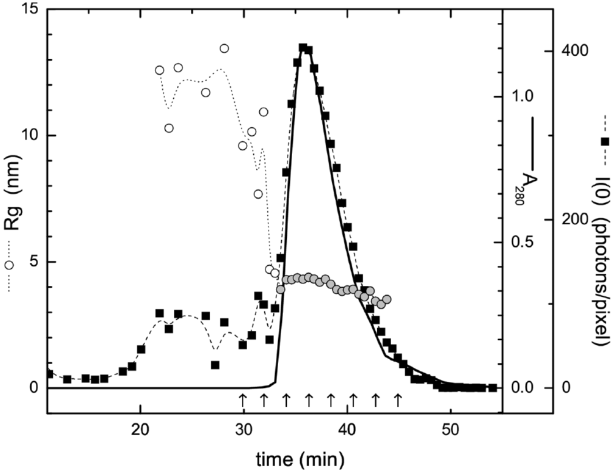

"Liquid-chromatography-coupled SAXS for accurate sizing of aggregating proteins," Mathew, Mirza & Menhart, *J. Synchrotron Rad.* **11**, 314-318 (2004).

Plasminogen

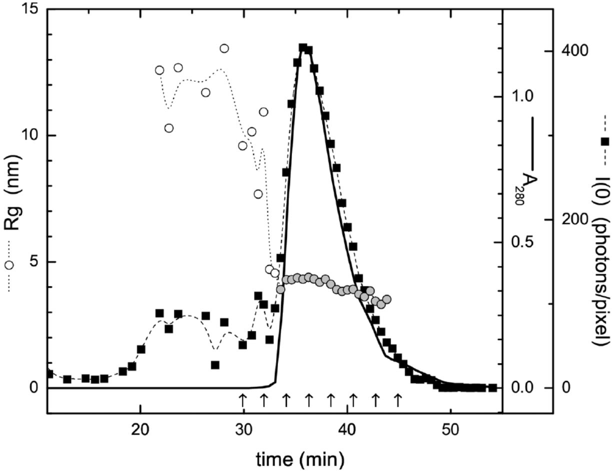

Constant R_g in regoin where $A_{UV}/I(0)$ is constant.

"Liquid-chromatography-coupled SAXS for accurate sizing of aggregating proteins," Mathew, Mirza & Menhart, *J. Synchrotron Rad.* **11**, 314-318 (2004).

Plasminogen

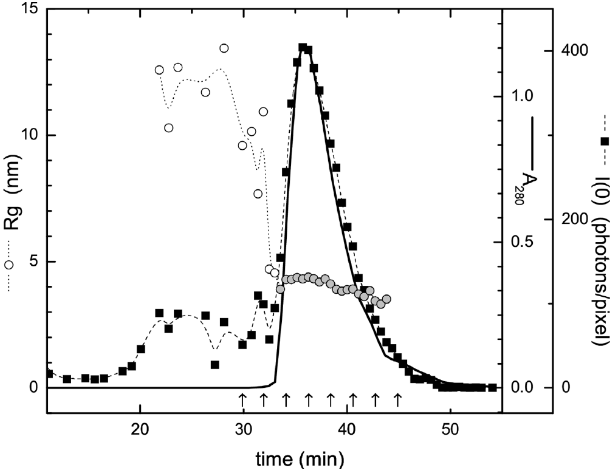

Constant R_g in regoin where $A_{UV}/I(0)$ is constant. Aggregates preceed the main peak and show wildly varying R_g.

"Liquid-chromatography-coupled SAXS for accurate sizing of aggregating proteins," Mathew, Mirza & Menhart, *J. Synchrotron Rad.* **11**, 314-318 (2004).

Plasminogen - Guinier plots

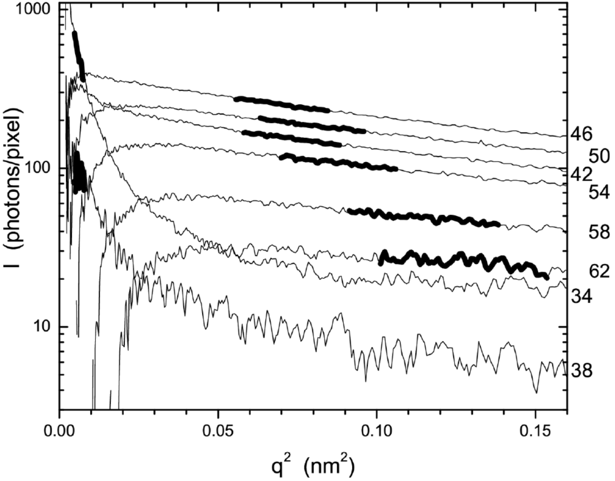

"Liquid-chromatography-coupled SAXS for accurate sizing of aggregating proteins," Mathew, Mirza & Menhart, *J. Synchrotron Rad.* **11**, 314-318 (2004).

Plasminogen - Guinier plots

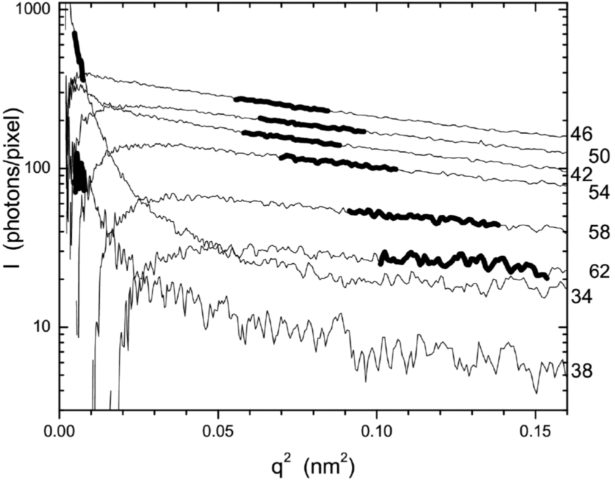

Guinier plots labeled 34 and 38 show presence of aggregates and the slopes are not parallel, indicating multiple sized species

"Liquid-chromatography-coupled SAXS for accurate sizing of aggregating proteins," Mathew, Mirza & Menhart, *J. Synchrotron Rad.* **11**, 314-318 (2004).

Three component mixture

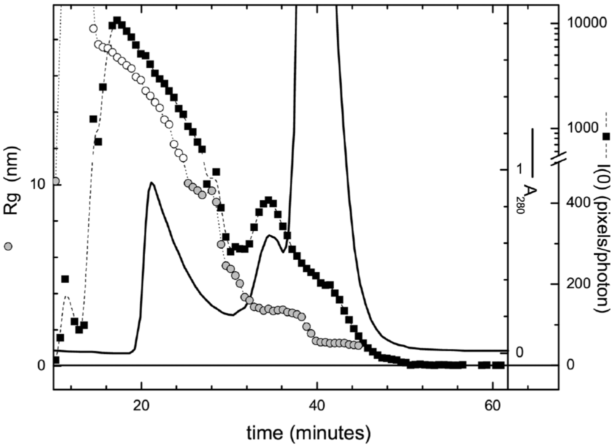

"Liquid-chromatography-coupled SAXS for accurate sizing of aggregating proteins," Mathew, Mirza & Menhart, *J. Synchrotron Rad.* **11**, 314-318 (2004).

Three component mixture

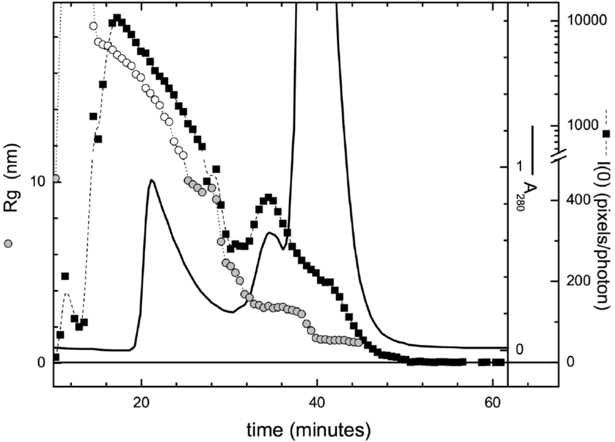

Tow the three components show consistent R_g and can be individually identified despite the overlap.

"Liquid-chromatography-coupled SAXS for accurate sizing of aggregating proteins," Mathew, Mirza & Menhart, *J. Synchrotron Rad.* **11**, 314-318 (2004).

Porosity in CaO calcination

SAXS was used to study the nature of the porosity and particle sizes of CaO obtained by calcining $CaCO_3$.

"Analysis of textural properties of CaO-based CO_2 sorbents by ex-situ USAXS," A. Benedetti, J. Ilavsky, C.U. Segre, and M. Strumendo, *Chem. Eng. J.* **355**, 760-776 (2019).

Porosity in CaO calcination

SAXS was used to study the nature of the porosity and particle sizes of CaO obtained by calcining $CaCO_3$.

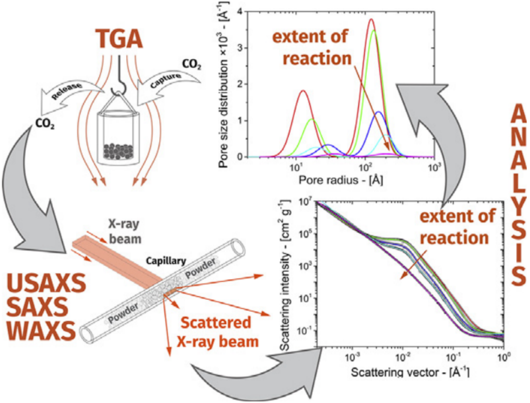

"Analysis of textural properties of CaO-based CO_2 sorbents by ex-situ USAXS," A. Benedetti, J. Ilavsky, C.U. Segre, and M. Strumendo, *Chem. Eng. J.* **355**, 760-776 (2019).

Porosity in CaO calcination

SAXS was used to study the nature of the porosity and particle sizes of CaO obtained by calcining $CaCO_3$.

CaO can be used for carbon capture and then recycled by calcination. It is important to understand the meso structure of the material at different stages of the process

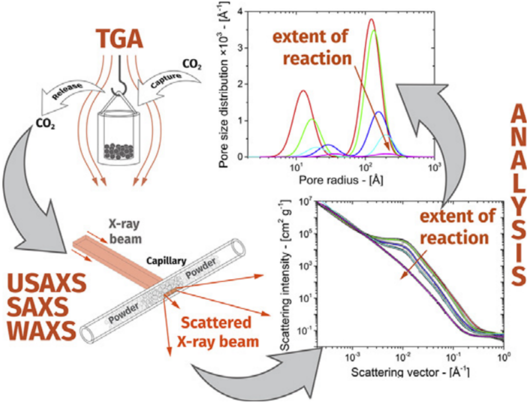

"Analysis of textural properties of CaO-based CO_2 sorbents by ex-situ USAXS," A. Benedetti, J. Ilavsky, C.U. Segre, and M. Strumendo, *Chem. Eng. J.* **355**, 760-776 (2019).

Porosity in CaO calcination

SAXS was used to study the nature of the porosity and particle sizes of CaO obtained by calcining $CaCO_3$.

CaO can be used for carbon capture and then recycled by calcination. It is important to understand the meso structure of the material at different stages of the process

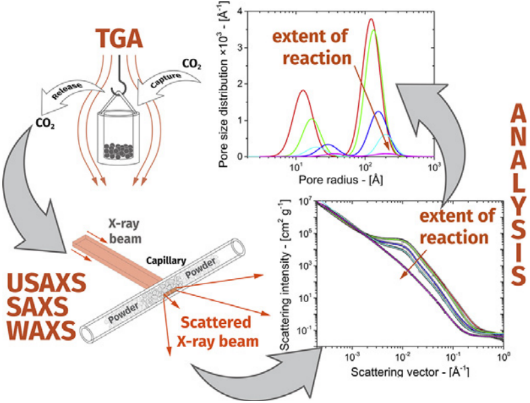

The samples were studied ex-situ at Sector 9-ID using USAXS and anyalyzed with a unified fit model

"Analysis of textural properties of CaO-based CO_2 sorbents by ex-situ USAXS," A. Benedetti, J. Ilavsky, C.U. Segre, and M. Strumendo, *Chem. Eng. J.* **355**, 760-776 (2019).

Porosity in CaO calcination

Sample D was calcined at 900 °C for 50 minutes while sample E was calcined at the same temperature for 240 minutes

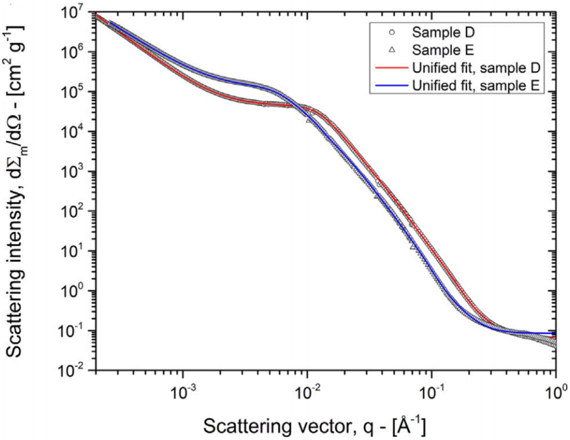

"Analysis of textural properties of CaO-based CO_2 sorbents by ex-situ USAXS," A. Benedetti, J. Ilavsky, C.U. Segre, and M. Strumendo, *Chem. Eng. J.* **355**, 760-776 (2019).

Porosity in CaO calcination

Sample D was calcined at 900 °C for 50 minutes while sample E was calcined at the same temperature for 240 minutes

The SAXS shows the grain growth evolution between the two samples and it is clear that the samples need a multilevel unified fit

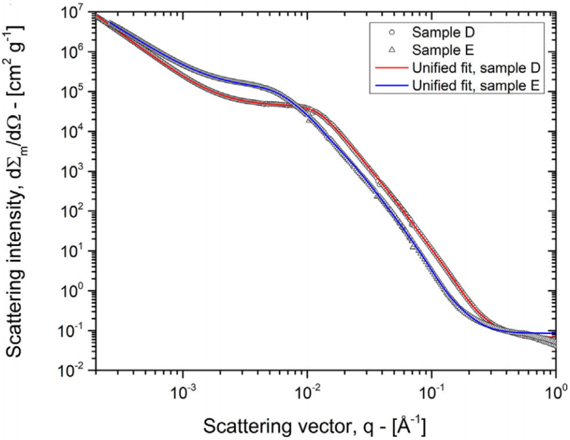

"Analysis of textural properties of CaO-based CO_2 sorbents by ex-situ USAXS," A. Benedetti, J. Ilavsky, C.U. Segre, and M. Strumendo, *Chem. Eng. J.* **355**, 760-776 (2019).

Porosity in CaO calcination

The components of the unified fit model are shown for a two level fit and it is clear that 2 levels are insufficient.

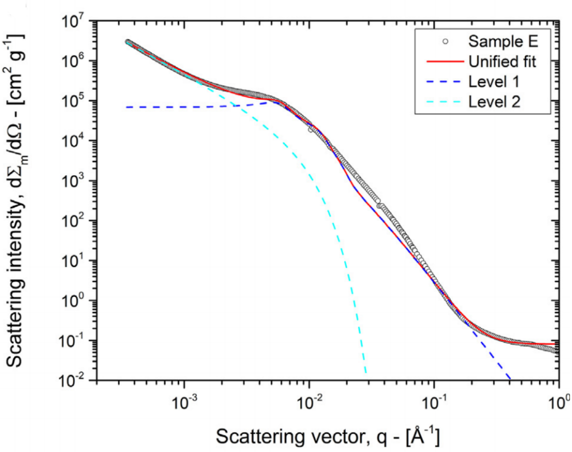

"Analysis of textural properties of CaO-based CO_2 sorbents by ex-situ USAXS," A. Benedetti, J. Ilavsky, C.U. Segre, and M. Strumendo, *Chem. Eng. J.* **355**, 760-776 (2019).

The components of the unified fit model are shown for a two level fit and it is clear that 2 levels are insufficient.

A three level fit works well for the calcined samples and from this one can extract the pore sized for two different pore populations in the calcined samples

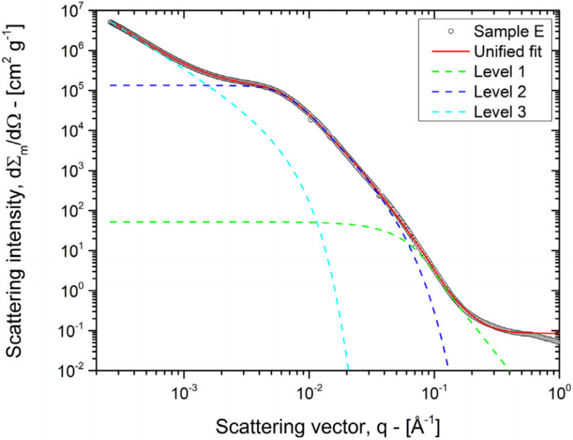

"Analysis of textural properties of CaO-based CO_2 sorbents by ex-situ USAXS," A. Benedetti, J. Ilavsky, C.U. Segre, and M. Strumendo, *Chem. Eng. J.* **355**, 760-776 (2019).

Porosity in CaO calcination

Fitting a series of samples calcined at varying temperatures and times shows the evolution of the radii of gyration of the two populations corresponding to the pore sizes

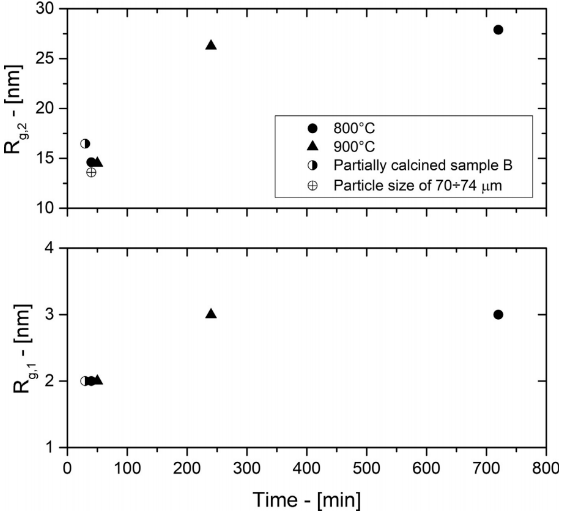

"Analysis of textural properties of CaO-based CO_2 sorbents by ex-situ USAXS," A. Benedetti, J. Ilavsky, C.U. Segre, and M. Strumendo, *Chem. Eng. J.* **355**, 760-776 (2019).

Porosity in CaO calcination

Fitting a series of samples calcined at varying temperatures and times shows the evolution of the radii of gyration of the two populations corresponding to the pore sizes

The resulting pore size distributions correspond well to those measured using gas adsorption methods

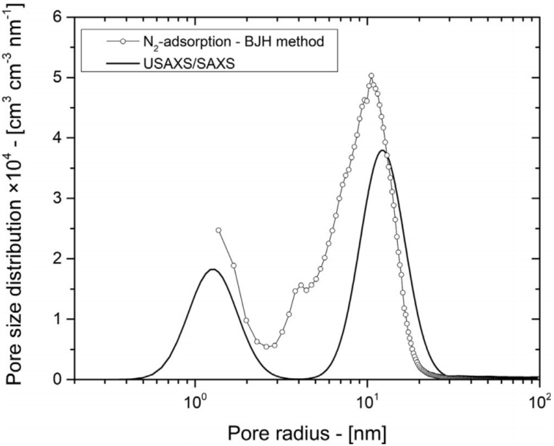

"Analysis of textural properties of CaO-based CO_2 sorbents by ex-situ USAXS," A. Benedetti, J. Ilavsky, C.U. Segre, and M. Strumendo, *Chem. Eng. J.* **355**, 760-776 (2019).